

Infrared Spectra and Theoretical Calculations of KH and (KH)₂ in Solid Hydrogen[†]

Xuefeng Wang and Lester Andrews*

Department of Chemistry, P. O. Box 400319, University of Virginia, Charlottesville, Virginia 22904-4319

Received: June 13, 2007; In Final Form: August 31, 2007

A matrix isolation IR study of laser-ablated potassium atom reactions with H₂ has been performed in solid molecular hydrogen. The KH molecule and (KH)₂ cluster were identified by infrared spectra with isotopic substitution (HD and D₂) and by comparison to frequencies calculated using density functional theory. In *para*-hydrogen, the sharp KH absorption suggests dihydrogen complex formation with the ionic KH molecule, which is also characterized by an absorption at 4095 cm⁻¹. The highly ionic rhombic (KH)₂ molecule is formed by dimerization and trapped in solid hydrogen. Calculations at the CCSD(T) level of theory show the increasing ionic character and decreasing stability for the (MH)₂ molecule series from Li to Cs.

Introduction

Alkali metal hydrides are an interesting contrast to their alkali metal halide counterparts. First, the solid hydrides are unstable and decompose to the elements, but the halides are very stable and evaporate stable molecules and oligomers. In fact, the thermal stability of the alkali metal hydrides decreases Li to Cs such that the temperature for reversible dissociation to H₂ (10 Torr) decreases from about 550 °C for Li to 170 °C for Cs.^{1–5} Second, the alkali metal hydride and halide dimers are highly ionic, and both have rhombus structures.^{6,7} Third, the alkali hydrides become even less stable as the metal size increases such that the equilibrium yield of KH in the presence of K and H₂ in the gas phase is insufficient for experimental investigations, and arc discharges have been employed for the early emission work and the diode laser infrared spectrum of KH.^{3,8} As a result, the dimerization energy decreases with metal size⁷ and the heavier alkali hydride dimers will be difficult to prepare for spectroscopic investigation.

To overcome the unfavorable thermodynamic situation, we have employed the reaction of laser-ablated lithium and sodium atoms with pure condensing hydrogen and trapped the LiH and NaH molecules in solid hydrogen. The use of ortho and *para*-hydrogen mixtures suggested that weak bisdihydrogen complexes (HH)₂MH with side-bound dihydrogen are trapped, and differences in the ortho or para spin state of the ligands were manifest in the complex vibrational spectra.^{9,10} Subsequent irradiation of these solid samples promoted the Li₂* and Na₂* reaction with the matrix host and led directly to the formation of (LiH)₂ and (NaH)₂. We report here a parallel investigation with potassium and the first experimental evidence for (KH)₂.

Experimental and Computational Methods

The experimental approach for reacting laser-ablated alkali metal atoms with condensing hydrogen has been described in previous research reports and one review article.^{9–11} Potassium metal is very soft and volatile, and care must be taken to apply the necessary laser energy and focus to ablate the proper amount of metal in order to carry out the desired potassium atom and small molecule chemistry. The Nd:YAG laser fundamental

[1064 nm, 10 Hz repetition rate, 10 ns pulse width, about 1 mJ/pulse] was focused onto a potassium metal target (freshly cut 10 × 10 × 5 mm piece, reagent grade) mounted on a rod and rotated at 1 rpm. Infrared spectra were recorded at 0.5 cm⁻¹ resolution and 0.1 cm⁻¹ accuracy on a Nicolet 750 using a Hg–Cd–Te range B detector. Matrix samples were annealed and irradiated by a medium-pressure mercury arc lamp (Osram Sylvania, 175 W) with the globe removed. Supporting electronic structure calculations were performed using the Gaussian 03 program system, the B3LYP density functional or the CCSD(T) method, and the 6-311++G(3df,3pd) basis sets.¹²

Results and Discussion

Infrared spectra will be presented for potassium atom reaction products with pure hydrogen, and infrared spectra for new potassium hydride cluster species will be assigned and substantiated through comparison with vibrational frequencies calculated by density functional theory. Absorptions were observed for hydrogen species that are common to laser-ablated metal experiments with solid hydrogen, but no potassium oxide impurities were found in the spectra.^{13–15} In particular, the trapped H⁻ anion complex absorption was very strong in potassium experiments. New results are also presented for the H–H stretching region in the lithium experiments.

Infrared Spectra. Two laser-ablated potassium deposits in pure condensing *normal*-hydrogen were investigated, and the spectrum of one of these is shown in Figure 1. The initial spectrum revealed new site-split doublets 4102.7, 4094.3 cm⁻¹ and 930.2, 918.6 cm⁻¹ [labeled (H₂)_nKH], and a weak broad band at 628 cm⁻¹ [labeled (KH)₂]. Irradiation of the sample with UV light >320 nm sharpened and increased the doublets slightly, 240–380 nm almost destroyed these peaks, and >220 nm eliminated them completely while the broad 628 cm⁻¹ band remained unchanged. Excimer irradiation at 193 nm had no effect. The weak 848 cm⁻¹ band destroyed on irradiation is not identified. Annealing in the second experiment produced no changes in the spectrum. A similar investigation with *normal*-deuterium gave only a weak band at 672.0 cm⁻¹ with no detectable absorption in the 450 cm⁻¹ region, which has poor signal-to-noise because of detector response. The 672.0 cm⁻¹ band increased substantially on >290 nm irradiation, which is

[†] Part of the "Giacinto Scoles Festschrift".

* Corresponding author. E-mail: lsa@virginia.edu.

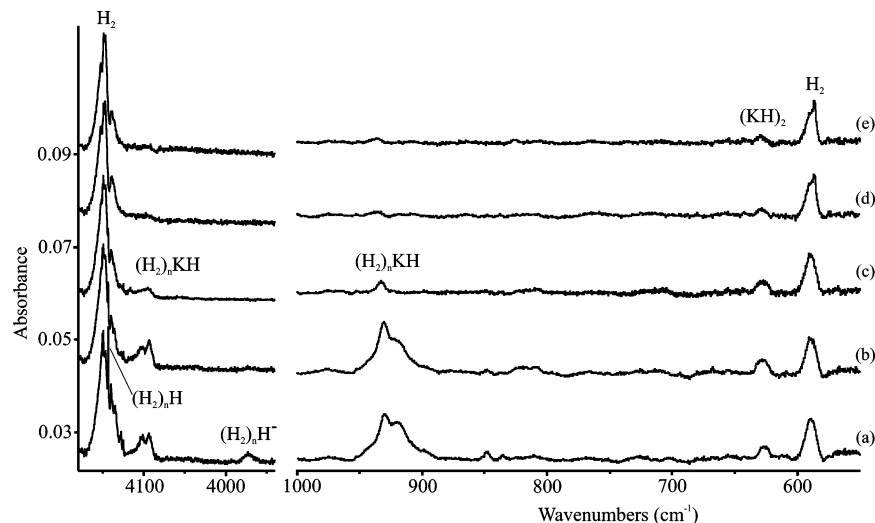


Figure 1. Infrared spectra for laser-ablated potassium atom reaction products with hydrogen. (a) Spectrum after co-deposition of laser-ablated potassium atoms and hydrogen gas for 30 min at 4 K, (b) after >320 nm irradiation, (c) after 240–380 nm irradiation, (d) after >220 nm irradiation, and (e) after 193 nm irradiation. The 588 cm⁻¹ band is due to solid hydrogen.

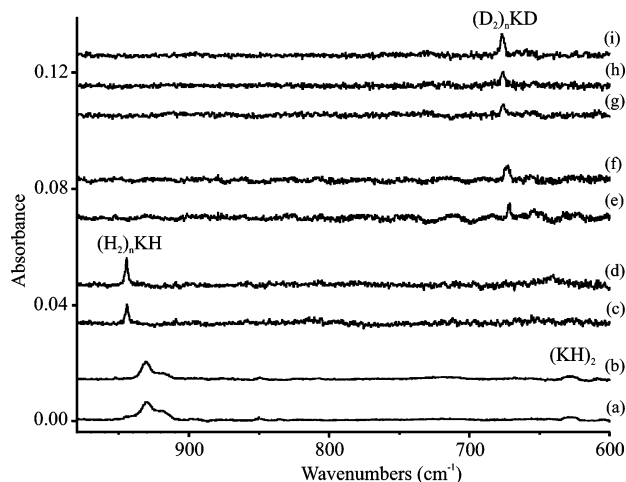


Figure 2. Infrared spectra for potassium atom reaction products with different quantum state hydrogen matrix samples. (a) Spectrum after co-deposition of laser-ablated potassium atoms and *normal*-hydrogen gas for 30 min at 4 K, (b) after >320 nm irradiation, (c) spectrum after co-deposition of K and 99.9% *para*-hydrogen for 20 min, (d) after >320 nm irradiation, (e) spectrum after co-deposition of K and *normal*-deuterium for 30 min, (f) after >290 nm irradiation, (g) spectrum after co-deposition of K and 98% *ortho*-deuterium for 20 min, (h) after >420 nm irradiation, and (i) after >290 nm irradiation.

illustrated in Figure 2e and f. A deposit with HD gave a doublet at 924.1, 919.4 cm⁻¹ for KH and a weak, broad 656 cm⁻¹ absorption.

Two experiments with 99.9% *para*-hydrogen^{16,17} produced a weak 4095.5 cm⁻¹ absorption and a sharp band at 944.4 cm⁻¹, which also increased on >320 nm irradiation (Figure 2). Potassium studies with 98% *ortho*-deuterium produced a sharp, weak 676.0 cm⁻¹ absorption, which increased on >420 nm and on >290 nm irradiation (Figure 2). A weak associated band appeared at 2940 cm⁻¹ during the irradiation cycles.

A final investigation with potassium and hydrogen in excess neon failed to give product absorptions.

Spectra from the H–H stretching region for the analogous lithium atom reactions in solid hydrogen are reported in Figure 3.

Calculations. The B3LYP hybrid density functional and large Gaussian basis set gave a 2.242 Å bond distance and 976.9 cm⁻¹

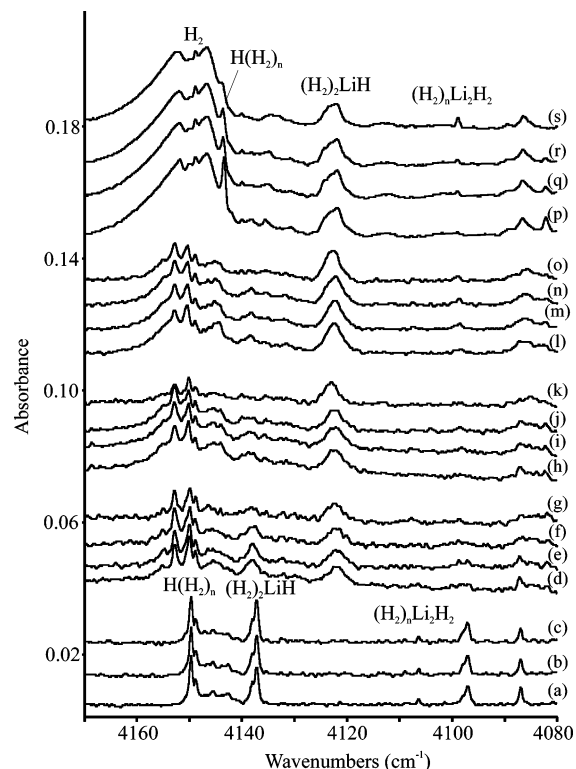


Figure 3. Infrared spectra for lithium atom reaction products with different *para* enriched hydrogen matrix samples. (a) Spectrum after co-deposition of laser-ablated lithium atoms and 99.9% *para*-hydrogen for 30 min at 4 K, (b) spectrum after annealing to 6.0 K, (c) after annealing to 6.5 K. (d) Spectra for Li with 99% *para*, and (e–g) after annealing to 6.0, 6.5, 6.7 K. (h) Spectra for Li with 90% *para*, and (i–k) after similar annealing cycles. (l) Spectra for Li with 70% *para*, and (m–o) spectra after similar annealing cycles. (p) Spectrum after co-deposition of Li and *normal*-hydrogen for 30 min, (q–s) spectra after >530, 470, and 380 nm irradiations.

harmonic frequency for the KH diatomic molecule. These may be compared with virtually the same experimental bond length and the measured 983.6 cm⁻¹ harmonic frequency and the infrared observed 955.9 cm⁻¹ vibrational frequency.⁸ Next, the (KH)₂ dimer was computed and the structure is given in Figure 4 with structures for (KF)₂ and (KCl)₂. Our B3LYP bond distance may be compared with the 2.473 Å value⁷ using the

TABLE 1: Observed and Calculated Frequencies (cm^{-1}) for $(\text{KH})_2$ Isotopic Molecules (1A_g in D_{2h} Symmetry)

mode	$(\text{KH})_2$		$(\text{KD})_2$		(KHKD)		
	obs ^a	calc harm ^b	obs	calc harm	mode	obs	calc harm
(b_{2u})		775(1007)		555(516)	(a_1)		723(443)
(a_g)		763(0)		542(0)	(a_1)	656	721(667)
(b_{1u})	628	668(1203)	n. o.	478(617)	(b_2)		503(467)
(b_{3g})		635(0)		455(0)	(b_2)		488(95)
(b_{3u})		340(863)		244(442)	(b_1)		295(653)
(a_g)		145(0)		145(0)	(a_1)		145(0)

^a Observed frequencies from solid H_2 . ^b Calculated harmonic frequencies at the B3LYP/6-311++G(3df,3pd) level of theory with infrared intensities in km/mol .

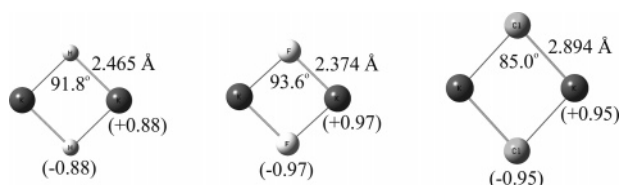


Figure 4. Structures calculated for the rhombic $(\text{KH})_2$, $(\text{KF})_2$, and $(\text{KCl})_2$ molecules using the B3LYP/6-311++G(3df,3pd) method. Bond lengths in Å and bond angles in degrees. Natural atomic charges are given for the cation and anion in each dimer molecule.

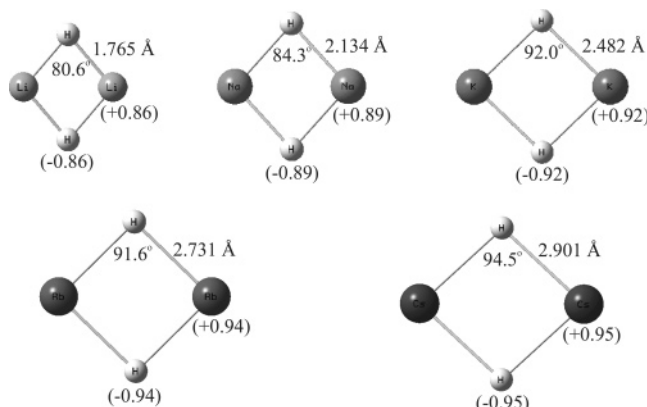
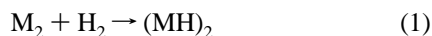


Figure 5. Structures calculated for the rhombic alkali hydride $(\text{MH})_2$ molecules using the CCSD(T)/6-311++G(3df,3pd) method. Bond lengths in Å and bond angles in degrees. Natural atomic charges are given for the cation and anion in each dimer molecule.

MP2 method. The harmonic vibrational frequencies are listed in Table 1. Note a reversal in the two highest mode symmetries from that for the lighter alkali hydride dimers, which means that mode mixing will be different for KHKD compared to NaH-NaD .^{9,10}

Next we employed the CCSD(T) method, which is the benchmark calculation for small molecules,¹⁸ and the large basis as the highest level of theory available to us, and the 2.482 Å bond distance and 92.0° K–H–K angle are only slightly different from the density functional values. Figure 5 compares the structures calculated for the five $(\text{MH})_2$ molecules, and Figure 6 contrasts the two HOMO's containing the four valence electrons at constant electron density using the CCSD(T) method. We also calculated energies for the important reaction (1) in these experiments at the CCSD(T) level and found the following energies, -30, -2.0, +1.5, +5.9, and +6.0 kcal/mol, respectively, for the Li, Na, K, Rb, and Cs reactions. This clearly shows the trend of decreasing stability for the heavier alkali metal hydride dimers.



Binding energies were computed at the MP2 level for H_2 side bound to the metal center, and the binding energies for reaction 2 are 3.8, 3.0, and 2.5 kcal/mol for Li, Na, and K, respectively. The binding energies for two side-bound dihydrogen molecules are 6.6, 5.6, and 4.9 kcal/mol.



KH. The reaction of laser-ablated K and H_2 in pure hydrogen gave a new 930.2 cm^{-1} product absorption, which increased on near UV but disappeared with shorter wavelength UV irradiation. The D_2 counterpart in pure deuterium at 672.0 cm^{-1} defines a 1.384 KH/KD frequency ratio, which is slightly lower than the 1.396 harmonic frequency ratio. Our 930.2 cm^{-1} absorption is 25.9 cm^{-1} (or 2.7%) lower than the gas-phase 955.9 cm^{-1} fundamental frequency,⁸ and the assignment to KH follows. The analogous investigations for LiH and NaH found frequencies 4.3% and 2.1% lower in solid hydrogen than the gas-phase fundamental frequencies, respectively.^{9,10} We computed the natural charge¹⁹ on the K center to be +0.81 for this ionic molecule at the B3LYP level of theory. The KH molecule apparently photodissociates to atoms with >220 nm irradiation.

The laser-ablated potassium atom reaction in 99.9% *para*-hydrogen gave a sharper product band at 944.4 cm^{-1} , which is only red-shifted 11.5 cm^{-1} from the gas-phase band position. The analogous band was observed at 676.0 cm^{-1} in 98% *ortho*-deuterium. The KH/KD ratio in the quantum solids, 1.397, is similar to the above value in the normal solid molecular hydrogens.

Our previous work with LiH and NaH in *para*-hydrogen and *normal*-hydrogen has characterized primary bisdihydrogen chemical complexes in a physical cage of dihydrogen molecules, and replacing the *para* with the *ortho* isomer in the primary complex and in the matrix cage leads to a red shift.^{9,10} That model also applies to the KH observed in this work. The additional red shift as *para*-hydrogen is replaced by *ortho*-hydrogen in the *normal*-hydrogen sample is 14.2 cm^{-1} for KH, 13.0 cm^{-1} for NaH, and 24.0 cm^{-1} for LiH, which suggests a comparable interaction with dihydrogen in a $(\text{H}_2)_n\text{KH}$ complex for the heavier alkali hydrides. The 4094.3 cm^{-1} band is associated with the 930.2 cm^{-1} band by common behavior on irradiation and similar splittings likely because of local sites in the hydrogen matrix, and we assign it to the H–H ligand stretching mode in this complex. The *para*-hydrogen counterparts were 4095.5 and 944.4 cm^{-1} , which shifted to 2940.0 and 676.0 cm^{-1} with *ortho*-deuterium. The H/D frequency ratios, 1.393 and 1.397, respectively, are appropriate for H–H and K–H vibrational modes. Our MP2 calculation predicts the stronger of two H–H stretching fundamentals for a model $(\text{H}_2)_2\text{-KH}$ complex to fall 102 cm^{-1} lower than H_2 itself, which is compared with shifts calculated for other complexes in Table 2, and our 4094 cm^{-1} band is lower than the solid hydrogen fundamental by 56 cm^{-1} , which is in qualitative agreement. Similar agreement is found for the analogous 4122.7 cm^{-1} band (2963.6 cm^{-1} deuterium counterpart, H/D ratio 1.3911) observed for the $(\text{H}_2)_2\text{LiH}$ complex,⁹ which is predicted by MP2 to be 13 cm^{-1} higher than the present $(\text{H}_2)_2\text{KH}$ complex. The lithium complex mode is observed to be 28 cm^{-1} higher, which is acceptable for these model calculations for weak complexes.

The 14.2 cm^{-1} red shift in the K–H fundamental on going from *para* to *normal* solid hydrogen ligands arises from the stronger interaction of *ortho*-hydrogen ligand with the polar KH molecule in the $(\text{H}_2)_n\text{KH}$ complex, than the *para*-hydrogen

TABLE 2: Calculated and Observed Parameters for (HH)_nMH Complexes

	H–H		freq		shift ^a		bond		energy ^b		M–H		freq		shift ^c		obs ^d		obs ^e	
<i>n</i>	1	2	3	1	2	3	1	2	3	1	2	3	1	2	3	24	58			
Li	69	89	111	3.8	6.6	9.5	11	19	33	24	58									
Na		44		3.0	5.6		3	8		n. o.	24									
K	83	102		2.5	4.9		2	9		52	26									

^a Calculated harmonic H₂ frequency minus strongest calculated H–H frequency, cm⁻¹ of complex with *n* ligands MP2/6-311++G(3df,3pd) theory. ^b Calculated total binding energy of *n*H₂ to MH, kcal/mol. ^c Calculated harmonic MH frequency minus calculated M–H frequency of complex. ^d Shift observed for H–H frequency from *para*-hydrogen matrix value, 4152 cm⁻¹. ^e Shift observed for M–H frequency from gas phase to *para*-hydrogen matrix value. All calculated frequencies are harmonic.

ligand owing to the quadrupole moment for the ortho nuclear spin isomer (*J* = 1) that is absent for *para*-hydrogen (*J* = 0).^{9,10,16,17,20} This small 14.2 cm⁻¹ shift for different dihydrogen spin state ligands is a small fraction of the total shift (Table 2) from isolated H₂ to the ligand in the complex with the polar KH molecule. Recently, this behavior has been clearly demonstrated and discussed for CH₃F.²⁰

The (H₂)_nKH complex is presumed to contain dihydrogen ligands side-bonded to the metal cation center, based on our computations for the analogous lithium species. Evidence has been presented for a bisdihydrogen lithium hydride complex and the computed structure illustrated,⁹ but we cannot determine definitively the number of ligands in the present KH complex by experiment or computation. Previous work involving dihydrogen complexes with alkali halides in argon and neon matrices has concluded that the dihydrogen frequency shift is greater for interaction with the anion than the cation center.^{21–24} Our calculations found that H₂ is bound more strongly to the Li than the H center in the polar LiH molecule.⁹ In the case of KF and H₂ in solid neon at 6–8 K, the most dilute sample gave a 4015 cm⁻¹ band, which was assigned to KF(H₂), and additional broader features appeared in the 4050–4100 cm⁻¹ region with higher H₂ concentrations.²⁴ This conclusion suggests that the higher frequency bands are due to H₂ ligands coordinated at the cation center, which is consistent with our observation of a 4094.3 cm⁻¹ band in *normal*-hydrogen and a 4095.5 cm⁻¹ band in *para*-hydrogen for the (H₂)_nKH complex.

The KH product is formed here using the same mechanism proposed in the gas-phase electrical discharge work,⁸ namely, the reaction of excited K atoms, reaction 2. Here the K atom reagent is electronically and/or thermally excited in the laser-ablation process. It also appears that near UV irradiation of the cold sample initiates this reaction. In addition, we observe perturbed H–H absorptions for trapped H atoms and hydride anion-solid hydrogen complexes, and the hydride anion complex absorption is particularly strong with potassium.^{13,14}



Analysis of the Hydrogen Region for Li and Na in Solid Hydrogen. The simple spectrum for K in the H₂ region (Figure 1) prompted further attempt to analyze the spectrum recorded for lithium.⁹ The Li–H stretching region revealed three bands for complexes with different numbers of *para* and *ortho* ligands, and this suggested two equivalent dihydrogen ligands in the (H₂)₂LiH complex. In addition to the known absorptions of hydrogen and the sharp features at 4151.8 cm⁻¹ (in *p*-H₂) and 4143.4 cm⁻¹ (in *n*-H₂) assigned to H(H₂)_n species,¹³ we observed a sharp new band at 4137.2 cm⁻¹ (Figure 3a for *p*-H₂) and a broader feature at 4122.4 cm⁻¹ (Figure 3p for *n*-H₂). These new bands track with the LiH stretching fundamental and can be assigned to the (H₂)₂LiH complex. The (D₂)₂LiD counterparts are found at 2967.7 and 2963.6 cm⁻¹ in *ortho*-deuterium and *normal*-deuterium, and the H/D frequency ratios are 1.3941 (*para*) and 1.3911 (*normal*). The absorptions in *para*-hydrogen and *ortho*-deuterium are shifted less owing to the weaker interaction for the *J* = 0 molecules as ligands. Notice how the absorption intensities change for the sets of spectra using 99, 90, and 70% *para*-hydrogen mixtures. The 99% *para* spectra revealed broader 4138.1 and 4123.1 cm⁻¹ bands of almost equal intensity on sample deposition (Figure 3d), but annealing (Figure 3e–g) decreased the upper band in favor of the lower band. The 90% *para* spectra revealed the same bands, but the upper band was much weaker and it decreased on annealing (Figure 3h–k). This trend continued in spectra from a 70% *para* sample (Figure 3l–o). Again we observe the replacement of the more weakly interacting *para* isomer by the more strongly interacting *ortho* isomer on changing *para* concentration and on annealing to allow exchange of *ortho*- for *para*-hydrogen in the sample.

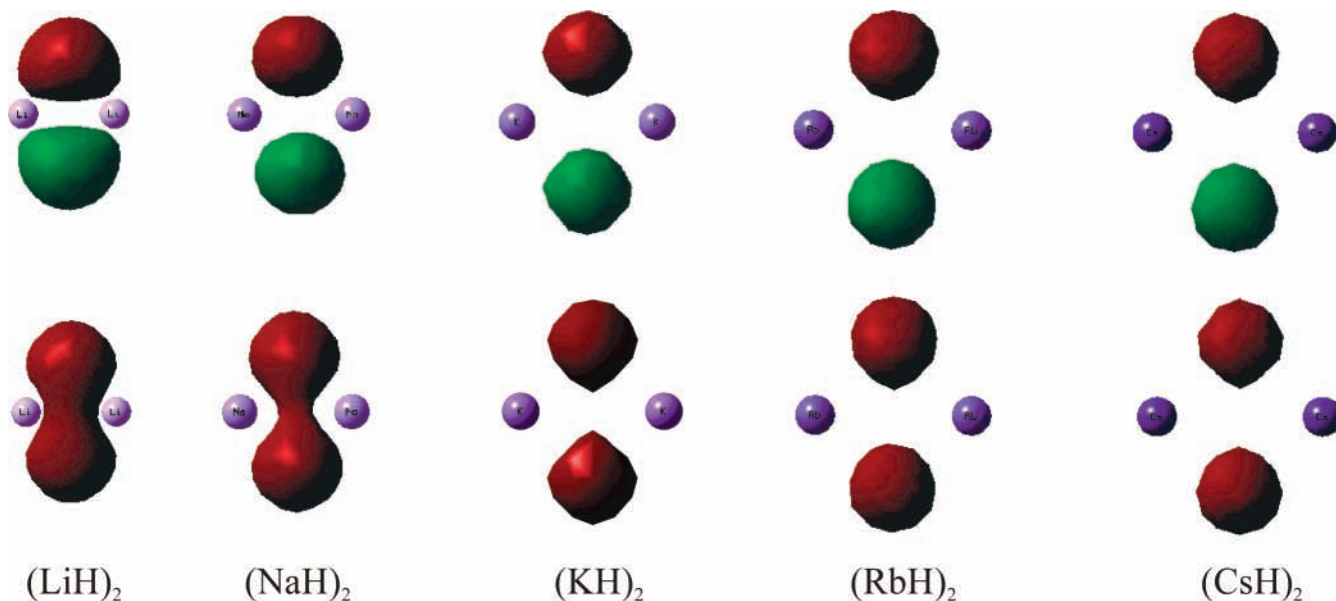


Figure 6. Two highest occupied molecular orbitals containing four valence electrons calculated for the alkali hydride (MH)₂ series using the CCSD(T) method. All plots are 0.05 e/au³ iso electron density level. The top is the highest energy MO.

The sharp, weak 4099.0 cm⁻¹ band in the *n*-H₂ sample tracks with the (LiH)₂ absorptions on annealing and irradiation, and it can be assigned to a dihydrogen ligand attached to the metal center in the (LiH)₂ molecule. The *para*-hydrogen counterpart is observed at 4106.4 cm⁻¹. Deuterium counterparts were found at 2946.4 and 2948.5 cm⁻¹, respectively, in *normal*- and *ortho*-deuterium, which define 1.3912 and 1.3927 H/D ratios. Other absorptions in the 3900–4100 cm⁻¹ region are decreased or destroyed on irradiation, and these are believed to be due to H₂ ligands on Li_{*n*} species that have no other infrared absorptions and cannot be readily identified. The analogous band for (NaH)₂ is observed at 4124.6 cm⁻¹, which appears on irradiation with the other fundamentals.¹⁰

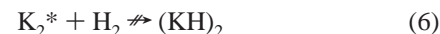
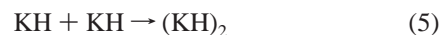
The Na experiment with *normal*-hydrogen gave additional sharp, weak 4130.2 and 4120.2 cm⁻¹ bands, which were destroyed on >320 nm irradiation as a new 4124.6 cm⁻¹ absorption appeared along with (NaH)₂ bands in the low-frequency region.¹⁰ Because the NaH absorption was constant during this procedure, the new band is associated with the (NaH)₂ molecule, and the 4130.2, 4120.2 cm⁻¹ bands with the (Na₂)(H₂)_{*n*} complex, which has no other IR absorption. No H–H stretching mode was observed for the (H₂)₂NaH complex, and our calculation finds it to be shifted less and likely not resolved from the solid hydrogen absorption.

Electronic structure calculations for the (HH)_{*n*}MH complexes are qualitatively in accord with this picture. The Li–H fundamental is shifted more than NaH and KH by the dihydrogen complex, and the H–H fundamental in (HH)_{*n*}KH is shifted more than the others. The MP2 level of theory is the highest that we can employ for these complexes (Table 2), but it overestimates the H–H ligand frequency shifts and underestimates the M–H frequency shifts. The binding energy of H₂ decreases as the alkali hydride becomes larger, as expected. We, of course, can only calculate the primary dihydrogen complexes without the effect of the dihydrogen matrix cage, which most likely contains an additional 12 weakly interacting molecules, and such a correction would be in the direction of improving the agreement between calculated and observed frequencies.

(KH)₂. The strongest infrared active fundamental for (KH)₂, the antisymmetric b_{1u} mode, is predicted at 668 cm⁻¹, and this mode is even stronger intensity-wise than the (LiH)₂ and (NaH)₂ counterparts as the computed natural charge on the metal center increases from +0.84 to +0.85 to +0.88 at the B3LYP level in the Li, Na, K series. The weak broad 628 cm⁻¹ absorption is assigned to this very strong mode for (KH)₂ based on the calculated frequency and scale factor 628/668 = 0.94 agreement with the 0.93 and 0.93 scale factors for the corresponding Li and Na species.^{9,10} Although the (KD)₂ absorption was not observed because of lower yield (also the case for Li and Na),^{9,10} the much stronger KHKD bands calculated at 722 and 723 cm⁻¹ are in accord with the weak, broad 656 cm⁻¹ absorption (scale factor 0.91). The yield of (KH)₂ in these experiments is much lower than what we found for the more favorable reactions with Li and Na, but this is dictated by the alkali metal chemistry, and we are fortunate to be able to detect (KH)₂ at all. The antisymmetric b_{2u} mode predicted at the B3LYP level at 775 cm⁻¹ with 84% of the infrared intensity of the b_{1u} mode is, unfortunately, not observed, with the low product yield. The calculation overestimates the intensity of the b_{2u} mode for this ionic molecule or the matrix diminishes its relative intensity. The same observation has been noted and discussed for (LiH)₂ and (NaH)₂.^{9,10}

The (KH)₂ observed here is formed by dimerization of KH, reaction 5, because irradiation failed to increase the product

yield, in contrast to the Li and Na cases. Reaction 5 is exothermic (–32 kcal/mol, B3LYP) but less so than the NaH (–33 kcal/mol) and LiH (–45 kcal/mol) dimerization reactions.^{9,10} We explored all UV excitation available to us, and surely we did excite K₂ into the analogous B state;³ but even so (KH)₂ is less stable than (NaH)₂, as shown by the above energy changes for reaction 1, which is less favorable for potassium. In addition, we probably had a much lower concentration of K₂ in our experiments.



Bonding. The highly ionic rhombic (KH)₂ molecule is like the isostructural (LiH)₂ and (NaH)₂ molecules, first observed in solid hydrogen where unfavorable thermodynamics can be overcome.^{1,5,9,10} In addition (KH)₂ is like the more stable and thus better-known potassium halide dimer structures⁶ (Figure 3). Note that the natural charges¹⁹ on the metal centers are +0.88, +0.97, and +0.95 for the (KH)₂, (KF)₂, and (KCl)₂ series calculated using the B3LYP hybrid density functional. The natural charges increase from +0.86 to +0.89 to +0.92 to +0.94 to +0.95 in the (LiH)₂ to (NaH)₂ to (KH)₂ to (RbH)₂ to (CsH)₂ series of highly ionic alkali hydride dimers based on calculations at the more rigorous CCSD(T) level of theory (Figure 5). Furthermore, the HOMO's containing the four valence electrons at constant electron density for each dimer (Figure 6) show the expected increase in ionic character on going down the alkali metal family.

Conclusions

Laser-ablated potassium atoms reacted with hydrogen gas during condensation at 4 K to form the KH diatomic molecule. This molecule is trapped as a dihydrogen complex (H₂)_{*n*}KH in solid hydrogen where the *para* and *ortho* spin states affect the H₂ and the KH absorption positions. *Ortho* and *para* dependence is also found for the (H₂)₂LiH complex.

The highly ionic potassium hydride dimer (KH)₂ is produced by dimerization and detected though the strongest infrared absorption at 628 cm⁻¹ in solid *normal*-hydrogen. The (MH)₂ molecules are highly ionic, and calculations at the CCSD(T) level of theory give the trend of natural charges on the metal centers increasing from +0.86 for (LiH)₂ to +0.95 for (CsH)₂. The HOMO's containing the four valence electrons for the alkali metal hydride series also show this expected increase in ionic character.

Acknowledgment. We gratefully acknowledge support for this work from N.S.F Grant CHE 03-52487.

References and Notes

- (1) (a) James, T. C.; Norris, W. G.; Klemperer, W. *J. Chem. Phys.* **1960**, *32*, 728. (b) Klemperer, W.; Norris, W. G. *J. Chem. Phys.* **1961**, *34*, 1071.
- (2) *Alkali Halide Vapors*; Davidovits, P., McFadden, D. L., Eds, Academic Press: New York, 1979.
- (3) Huber, K. P.; Herzberg, G. *Constants of Diatomic Molecules*; Van Nostrand-Reinhold: New York, 1979.
- (4) Greenwood, N. N.; Earnshaw, A. *Chemistry of the Elements*, 2nd ed.; Butterworth-Heinemann Ltd.: U. K., 2004.
- (5) Sastry, K. V. L. N.; Herbst, E.; DeLucia, D. F. *J. Chem. Phys.* **1981**, *75*, 4753 and references therein.
- (6) Dickey, R. P.; Maurice, D.; Cave, R. J. Mawhorter, R. *J. Chem. Phys.* **1993**, *98*, 2182.
- (7) Kremer, T.; Harder, S.; Junge, M.; Schleyer, P. v. R. *Organometallics* **1996**, *15*, 585.

- (8) Haese, N. N.; Liu, D.-J.; Altman, R. S. *J. Chem. Phys.* **1984**, *81*, 3766 and references therein.
- (9) (a) Wang, X.; Andrews, L. *Angew. Chem.* **2007**, *119*, 46, 2602. (b) Wang, X.; Andrews, L. *J. Phys. Chem. A* **2007**, *111*, 6008 (Li + H₂). Examination of the high-frequency region reveals a 4122.7 cm⁻¹ band that tracks with the LiH fundamental and can be assigned to the (H₂)₂LiH complex. The (D₂)₂LiD counterpart is found at 2963.6 cm⁻¹. These bands are observed at 4137.2 and 2967.7 cm⁻¹ in *para*-hydrogen and *ortho*-deuterium, which are shifted less owing to the weaker interaction for the *J* = 0 molecules.
- (10) Wang, X.; Andrews, L. *J. Phys. Chem. A* **2007**, *111*, 7098 (Na + H₂).
- (11) Andrews, L. *Chem. Soc. Rev.* **2004**, *33*, 123 and references therein.
- (12) Frisch, M. J.; Trucks, G. W.; Schlegel, H. B.; Scuseria, G. E.; Robb, M. A.; Cheeseman, J. R.; Montgomery, J. A., Jr.; Vreven, T.; Kudin, K. N.; Burant, J. C.; Millam, J. M.; Iyengar, S. S.; Tomasi, J.; Barone, V.; Mennucci, B.; Cossi, M.; Scalmani, G.; Rega, N.; Petersson, G. A.; Nakatsuji, H.; Hada, M.; Ehara, M.; Toyota, K.; Fukuda, R.; Hasegawa, J.; Ishida, M.; Nakajima, T.; Honda, Y.; Kitao, O.; Nakai, H.; Klene, M.; Li, X.; Knox, J. E.; Hratchian, H. P.; Cross, J. B.; Bakken, V.; Adamo, C.; Jaramillo, J.; Gomperts, R.; Stratmann, R. E.; Yazyev, O.; Austin, A. J.; Cammi, R.; Pomelli, C.; Ochterski, J. W.; Ayala, P. Y.; Morokuma, K.; Voth, G. A.; Salvador, P.; Dannenberg, J. J.; Zakrzewski, V. G.; Dapprich, S.; Daniels, A. D.; Strain, M. C.; Farkas, O.; Malick, D. K.; Rabuck, A. D.; Raghavachari, K.; Foresman, J. B.; Ortiz, J. V.; Cui, Q.; Baboul, A. G.; Clifford, S.; Cioslowski, J.; Stefanov, B. B.; Liu, G.; Liashenko, A.; Piskorz, P.; Komaromi, I.; Martin, R. L.; Fox, D. J.; Keith, T.; Al-Laham, M. A.; Peng, C. Y.; Nanayakkara, A.; Challacombe, M.; Gill, P. M. W.; Johnson, B.; Chen, W.; Wong, M. W.; Gonzalez, C.; Pople, J. A. *Gaussian 03*, revision C.02; Gaussian, Inc.: Wallingford, CT, 2004, and references therein.
- (13) Andrews, L.; Wang, X. *J. Phys. Chem. A* **2004**, *108*, 3879. (H / H₂).
- (14) Andrews, L.; Wang, X. *J. Phys. Chem. A* **2004**, *108*, 1103. (H⁻ / H₂).
- (15) Andrews, L. *J. Chem. Phys.* **1971**, *54*, 4935.
- (16) Silvera, I. F. *Rev. Mod. Phys.* **1980**, *52*, 393.
- (17) Andrews, L.; Wang, X. *Rev. Sci. Instr.* **2004**, *75*, 3039.
- (18) (a) Purvis, G. D.; Bartlett, R. J. *J. Chem. Phys.* **1982**, *76*, 1910. (b) Frisner, R. *Proc. Natl. Acad. Sci. U.S.A.* **2005**, *102*, 6648.
- (19) Reed, A. E.; Curtiss, L. A.; Weinhold, F. *Chem. Rev.* **1988**, *88*, 899.
- (20) (a) Yoshioka, K.; Anderson, D. T. *J. Chem. Phys.* **2003**, *119*, 4731 and references therein. (b) Yoshioka, K.; Anderson, D. T. *J. Mol. Struct.* **2006**, *786*, 123.
- (21) Ogden, J. S.; Rest, A. J.; Sweaney, R. L. *J. Phys. Chem.* **1995**, *99*, 8485.
- (22) Ogden, J. S.; Sweaney, R. L. *Inorg. Chem.* **1997**, *36*, 2523.
- (23) McKee, M. L.; Sweaney, R. L. *J. Phys. Chem. A* **2000**, *104*, 962.
- (24) Sweaney, R. L.; Vuong, L.; Bishara, J. *J. Phys. Chem. A* **2002**, *106*, 11440.